Acta Mech 214, 315–325 (2010)
DOI 10.1007/s00707-010-0293-x

M. M. Kamel · Y. S. Hamed

Nonlinear analysis of an elastic cable under harmonic excitation

Received: 28 August 2009 / Revised: 30 November 2009 / Published online: 21 March 2010

Abstract The nonlinear behavior of an elastic cable subjected to harmonic excitation is studied and solved. The method of multiple scales perturbation is applied to analyze the response of the nonlinear system near the simultaneous principle primary and internal resonance. The stability of the proposed analytic nonlinear solution near the simultaneous primary-internal resonance is studied and the stability condition is investigated. The effect of different parameters on the steady state responses of the vibrating system is studied and discussed using frequency response equations. The numerical solutions and chaotic response of the nonlinear system of the elastic cable for different parameters are also studied.

1 Introduction

Cables are very efficient structural members and hence have been widely used in many long-span structures, including cable-supported bridges, roofs and guyed towers. The dynamic study of the cable is very complicated and remains a key research field of mathematics, mechanics and engineering. Environmental excitations, such as wind, bridge traffic, rain–wind interaction…etc., may result in large amplitude cable vibrations. Such vibrations mainly involve the first in-plane and out-of-plane modes. The modal interactions and coupling phenomena may also involve higher-order modes, due to quadratic and cubic nonlinearities in the equations of motion. Zhao et al. [1] dealt with a two degree of freedom model of an inclined cable for a theoretical investigation of in-plane and out-of-plane modes motion approximated by the first in-plane and out-of-plane modes. Nielsen and Kierkegaard [2] investigated simplified models of inclined cables under super and combinatorial harmonic excitation and gave analytical and purely numerical results. Some interesting works on the nonlinear dynamics of cables to the harmonic excitations can be found in the review articles by Rega [3,4]. Moreover, the theoretical and experimental investigations of an inclined cable subjected to external sinusoidal forcing leading to primary and sub-harmonic resonances are studied by Berlioz and Lamarque [5]. Kamel et al. [6–9] studied different nonlinear systems subjected to external excitations, and the steady state solutions of these nonlinear systems are studied using multiple scales perturbation to solve the frequency response equations.

Many studies have been performed on large amplitude vibrations of cable structures, and many different methods to investigate the nonlinear dynamics have been applied. The nonlinear dynamics of cable structures to the harmonic excitations have been studied with one-to-one internal resonances by Zhao et al. [1]. Also, the nonlinear dynamics of these cable structures have been studied with two-to-one internal resonances by the authors [10–12] and studied with multiple internal resonances by the authors [13,14]. Lacarbonara and Rega [15] have studied the nonlinear interaction and large amplitude vibration of a suspend cable with a three-to-one internal resonance, which might be activated between the symmetric in-plane modes. Arafat and Nayfeh [16] studied also the motion of shallow suspended cables with primary resonance excitation.

M. M. Kamel · Y. S. Hamed (✉)
Department of Engineering Mathematics, Faculty of Electronic Engineering, Menouf 32952, Egypt
E-mail: eng_yaser_salah@yahoo.com

The method of multiple scales is applied to study nonlinear response of this suspended cables and its stability and the dynamic solutions. The nonlinear vibration of shallow cables with a semiactive tuned mass damper is considered and studied by Casciati and Ubertini [17]. A simple control algorithm is adopted to regulate the out-of-plane inclination, and the effectiveness of the proposed control is analyzed using numerical simulations of finite element methods. Results of both free and harmonically forced vibrations are presented. A theoretical discussion and some numerical results relating to a nonlinear state designed for shallow cable vibration are presented and studied by Faravelli and Ubertini [18]. A sample suspended cable, representing a physical model is considered as the case study, and noncollocated feedback, based on active transverse control, is considered as a final application of the state observer. Also, active feedback control for cable vibrations is studied by Ubertini [19] for analytical and numerical models. A suitable dimensional analytical Galerkin model is derived to investigate the effectiveness of the feedback control, which represents the final application of the state observer. Wang and Zhao applied different methods to investigate the nonlinear response of the suspend cable with three-to-one internal resonance, and numerical simulations are used to illustrate the chaotic dynamics of the cable [20–22]. They also extended the previous work to consider the out-of-plane motion of a shallow suspended cable [23]. The three-to-one internal resonance between the third and the first symmetric in-plane modes and the one-to-one internal resonance between the third symmetric in-plane mode and the third symmetric out-of-plane mode are taken into account. The case of the primary resonance of the first symmetric mode is also considered.

The object of this work deals with models having a two degree of freedom nonlinear system subjected to harmonic excitation and describes the vibrations of an inclined cable. The method of multiple scales perturbation [24,25] is applied to obtain modulation response equations near the simultaneous principle primary and internal resonance. The stability of the proposed analytic nonlinear solution near the simultaneous primary-internal resonances is studied and the stability condition is determined. The effect of different parameters on the steady state responses of the vibrating system is studied and discussed from the frequency response curves using Matlab scheme. The numerical solution and chaotic responses of the nonlinear system of the elastic cable for different parameters are also studied using Maple scheme.

2 Equations of motions

In this study, our attention is focused on an inclined-sag hanging at fixed supports and excited by harmonic distributed vertical forcing in plane. This plane is defined by the initial static configuration of the inclined cable and horizontal load as shown in Fig. 1.

Galerkin's method is applied to obtain a model with two degree of freedom nonlinear system subjected to external sinusoidal forcing [1,26]. This nonlinear system can be written as:

$$\ddot{X} + 2\varepsilon^2\mu_1\dot{X} + \omega_1^2 X + \varepsilon(\alpha_1 X^2 + \alpha_2 Y^2) + \varepsilon^2(\beta_1 X^3 + \beta_2 Y^3) = 0, \tag{1.1}$$

$$\ddot{Y} + 2\varepsilon^2\mu_2\dot{Y} + \omega_2^2 Y + \varepsilon(\alpha_3 XY) + \varepsilon^2(\beta_3 Y^3 + \beta_4 X^2 Y) = 2\varepsilon^2 f\cos\Omega t, \tag{1.2}$$

where X and Y are the displacements of the cable and dots denote derivatives with respect to time t. The parameters μ_1 and μ_2 are the viscous damping coefficients, ω_1 and ω_2 are the natural frequencies, Ω is the excitation frequency, f is the excitation force amplitude, $\alpha_1, \ldots, \alpha_3$ and $\beta_1, \ldots, \beta_4$ are the coefficients of nonlinear parameters and ε is a small perturbation parameter.

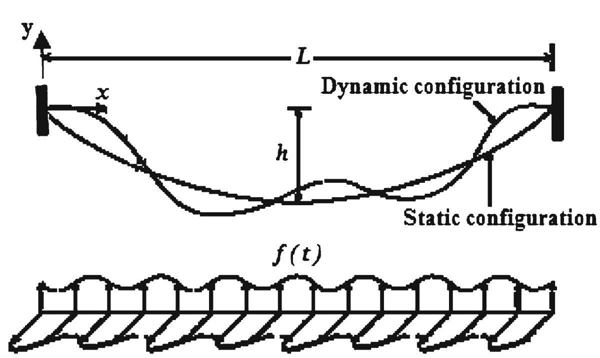

Fig. 1 A schematic of the elastic cable under external excitations

3 Perturbation analysis

The multiple scale perturbation method is conducted to obtain an approximation solution for Eq. (1). So, assuming the solution in the form:

$$X(t;\varepsilon) = x_0(T_0, T_1, T_2) + \varepsilon x_1(T_0, T_1, T_2) + \varepsilon^2 x_2(T_0, T_1, T_2) + \cdots, \tag{2.1}$$

$$Y(t;\varepsilon) = y_0(T_0, T_1, T_2) + \varepsilon y_1(T_0, T_1, T_2) + \varepsilon^2 y_2(T_0, T_1, T_2) + \cdots, \tag{2.2}$$

the time derivatives become

$$\frac{d}{dt} = D_0 + \varepsilon D_1 + \varepsilon^2 D_2, \quad \frac{d^2}{dt^2} = D_0^2 + 2\varepsilon D_0 D_1 + \varepsilon^2 D_1^2 + 2\varepsilon^2 D_1 D_2, \tag{3}$$

where $T_n = \varepsilon^n t$ $(n = 0, 1, 2)$ are the fast and slow time scales, respectively. Substituting Eqs. (2) and (3) into Eq. (1) and equating the coefficients of same powers of ε, we obtain the following:

$$(D_0^2 + \omega_1^2)x_0 = 0, \tag{4.1}$$

$$(D_0^2 + \omega_2^2)y_0 = 0, \tag{4.2}$$

$$(D_0^2 + \omega_1^2)x_1 = -2D_0D_1x_0 - \alpha_1 x_0^2 - \alpha_2 y_0^2, \tag{5.1}$$

$$(D_0^2 + \omega_2^2)y_1 = -2D_0D_1y_0 - \alpha_3 x_0 y_0, \tag{5.2}$$

$$\begin{aligned}(D_0^2 + \omega_1^2)x_2 = &-D_1^2x_0 - 2D_0D_1x_1 - 2D_0D_2x_0 - 2\mu_1 D_0 x_0 \\ &-2\alpha_1 x_0 x_1 - 2\alpha_2 y_0 y_1 - \beta_1 x_0^3 - \beta_2 x_0 y_0^2,\end{aligned} \tag{6.1}$$

$$\begin{aligned}(D_0^2 + \omega_2^2)y_2 = &-D_1^2y_0 - 2D_0D_1y_1 - 2D_0D_2y_0 - 2\mu_2 D_0 y_0 - \alpha_3(x_0y_1 + y_0x_1) \\ &-\beta_3 y_0^3 - \beta_4 y_0 x_0^2 + 2f\cos\Omega T_0.\end{aligned} \tag{6.2}$$

The general solution of Eq. (4) can be expressed in the form

$$x_0 = A_0 \exp(j\omega_1 T_0) + cc, \tag{7.1}$$

$$y_0 = B_0 \exp(j\omega_2 T_0) + cc, \tag{7.2}$$

where A_0 and B_0 are complex functions and cc denotes complex conjugate terms. Substituting Eq. (7) into Eq.(5) and eliminating the secular terms, the bounded first-order approximation yields

$$x_1 = A_1 \exp(j\omega_1 T_0) + E_1 \exp(2j\omega_1 T_0) - E_2 \exp(2j\omega_2 T_0) + c_1 + cc, \tag{8.1}$$

$$y_1 = B_1 \exp(j\omega_2 T_0) + E_3 \exp((\omega_2 + \omega_1)T_0) - E_4 \exp((\omega_2 - \omega_1)T_0) + cc. \tag{8.2}$$

From the elimination of secular terms we have $D_1A_0 = D_1B_0 = 0$, this means that A_0 and B_0 are only functions in T_2. Hence, $A_1, B_1, E_1, \ldots, E_4$ are complex conjugate functions in T_2.

Now substituting Eqs. (7) and (8) into Eq. (6), the following are obtained:

$$\begin{aligned}(D_0^2 + \omega_1^2)x_2 = &(-D_1^2A_0 - 2j\omega_1\mu_1A_0 - 2j\omega_1D_1A_1 - 2j\omega_1D_2A_0 - 2\alpha_1\bar{A}_0E_1 - 4\alpha_1c_1\bar{A}_0E_1 \\ &-2\alpha_2(\bar{B}_0E_3 - B_0\bar{E}_4) - 3\beta_1A_0^2\bar{A}_0 - 2\beta_2\bar{B}_0B_0A_0)\exp(j\omega_1T_0) + (-4j\omega_1D_1E_1 \\ &+2\alpha_1A_0A_1)\exp(2j\omega_1T_0) + (4j\omega_2D_1E_2 - 2\alpha_2B_0B_1)\exp(2j\omega_2T_0) - (2\alpha_1A_0E_1 \\ &+\beta_1A_0^3)\exp(3j\omega_1T_0) + (2\alpha_1A_0E_2 - 2\alpha_2B_0E_3 - \beta_2A_0B_0^2)\exp((2\omega_2 + \omega_1)T_0) \\ &+(2\alpha_1\bar{A}_0E_2 + 2\alpha_2B_0E_4 - \beta_2\bar{A}_0B_0^2)\exp((2\omega_2 - \omega_1)T_0) - (2\alpha_1A_0\bar{A}_0 + 2\alpha_2B_0\bar{B}_0) + cc,\end{aligned} \tag{9.1}$$

$$\begin{aligned}(D_0^2 + \omega_2^2)y_2 = &(-D_1^2B_0 - 2j\omega_2\mu_2B_0 - 2j\omega_2D_1B_1 - 2j\omega_2D_2B_0 - \alpha_3(\bar{A}_0E_3 - A_0E_4) \\ &-2\alpha_3c_1B_0 + \alpha_3E_2\bar{A}_0 - 3\beta_3B_0^2\bar{B}_0 - 2\beta_4A_0\bar{A}_0B_0)\exp(j\omega_2T_0) + (\alpha_3E_2B_0 \\ &-\beta_3B_0^3)\exp(3j\omega_2T_0) + f\exp(j\Omega T_0) + (-2j(\omega_2 + \omega_1)D_1E_3 - \alpha_3A_0B_1 \\ &-2\alpha_3A_1B_0)\exp((\omega_1 + \omega_2)T_0) + (2j(\omega_1 - \omega_2)D_1E_4 - \alpha_3A_0\bar{B}_1 - 2\alpha_3A_1\bar{B}_0) \\ &\times\exp((\omega_1 - \omega_2)T_0) + (-\alpha_3A_0E_3 - \alpha_3B_0E_1 - \beta_4B_0A_0^2)\exp((2\omega_1 + \omega_2)T_0) \\ &+(\alpha_3A_0\bar{E}_4 - \alpha_3\bar{B}_0E_1 - \beta_4\bar{B}_0A_0^2)\exp((2\omega_1 - \omega_2)T_0) + cc.\end{aligned} \tag{9.2}$$

From the simultaneous primary and internal resonance case (worst case) which is deduced from the solution of Eq. (9), we can introduce detuning parameters σ_1 and σ_2 such that

$$\omega_2 = \omega_1 + \varepsilon^2\sigma_1 \quad \text{and} \quad \Omega = \omega_2 + \varepsilon^2\sigma_2. \tag{10}$$

Substituting Eq. (10) into Eq. (9) and setting the coefficients of the secular terms to zero yields the solvability conditions as

$$A_0' + \mu_1 A_0 - jK_1 A_0^2\bar{A}_0 - jK_2 A_0 B_0 \bar{B}_0 - jL_1 \bar{A}_0 B_0^2 \exp(2j\sigma_1 T_2) = 0, \tag{11.1}$$

$$B_0' + \mu_2 B_0 - jK_3 B_0^2 \bar{B}_0 - jK_4 B_0 A_0 \bar{A}_0 - jL_2 \bar{B}_0 A_0^2 \exp(-2j\sigma_1 T_2) + jF\exp(j\sigma_2 T_2) = 0, \tag{11.2}$$

where, $K_1, \ldots, K_4$, L_1, L_2 and F are new constants (see "Appendix").

Introducing polar notation $A_0(T_2) = a(T_2)\exp(j\gamma_1(T_2))$ and $B_0(T_2) = b(T_2)\exp(j\gamma_2(T_2))$ into Eq. (11) and separating the real and imaginary parts yields the modulation equations

$$a' + \mu_1 a = -L_1 ab^2 \sin\theta_1, \tag{12.1}$$

$$a\gamma_1' - K_1 a^3 - K_2 ab^2 = L_1 ab^2 \cos\theta_1, \tag{12.2}$$

$$b' + \mu_2 b - F\sin\theta_2 = L_2 a^2 b \sin\theta_1, \tag{13.1}$$

$$b\gamma_2' - K_3 b^3 - K_4 ba^2 + F\cos\theta_2 = L_2 a^2 b\cos\theta_1, \tag{13.2}$$

where a and b are the steady state amplitudes, γ_1 and γ_2 are the phases of the motion and $\theta_1 = 2\sigma_1 T_2 + \gamma_2 - \gamma_1$ and $\theta_2 = \sigma_2 T_2 - \gamma_2$.

For steady state solutions we have $a' = b' = \theta_1' = \theta_2' = 0$, and they can be obtained from Eqs. (12) and (13) as follows:

$$\mu_1 = -L_1 b^2 \sin\theta_1, \tag{14.1}$$

$$(2\sigma_1 + \sigma_2) - \left(K_1 a^2 + K_2 b^2\right) = L_1 b^2 \cos\theta_1, \tag{14.2}$$

$$\mu_2 + \mu_1 L_2 \frac{a^2}{b^2} = \frac{F}{b}\sin\theta_2, \tag{15.1}$$

$$\sigma_2 - \left(K_3 b^2 + K_4 a^2\right) - L_2 a^2 \left(\frac{(2\sigma_1 + \sigma_2) - \left(K_1 a^2 + K_2 b^2\right)}{L_1 b^2}\right) = -\frac{F}{b}\cos\theta_2. \tag{15.2}$$

From Eqs. (14.1), (14.2) and (15.1), (15.2), the following frequency response equations can be obtained:

$$\sigma_1^2 + \left[\sigma_2 - \left(K_1 a^2 + K_2 b^2\right)\right]\sigma_1 + \frac{1}{4}\left[\sigma_2^2 - 2\sigma_2\left(K_1 a^2 + K_2 b^2\right) + \left(K_1 a^2 + K_2 b^2\right)^2 + \mu_1^2 - L_1^2 b^4\right] = 0, \tag{16}$$

$$\sigma_2^2 - 2\left[\left(K_3 b^2 + K_4 a^2\right) \pm \frac{L_2 a^2 \sqrt{L_1^2 b^4 - \mu_1^2}}{L_1 b^2}\right]\sigma_2 \left[\left(\left(K_3 b^2 + K_4 a^2\right) \pm \frac{L_2 a^2 \sqrt{L_1^2 b^4 - \mu_1^2}}{L_1 b^2}\right)^2 + \left(\mu_2 + \frac{\mu_1 L_2 a^2}{b^2}\right)^2 - \frac{F^2}{b^2}\right] = 0, \tag{17}$$

$$f^2 - \left(4\omega_2 L_2 a^2 b\right) f + 4\omega_2^2 \left(L_2^2 a^4 b^2 - b^2\mu_2^2 - \left(K_3 b^2 + K_4 a^2\right)^2 - b^2\sigma_2^2 + b^2\left(2K_3 b^2 + 2K_4 a^2\right)\sigma_2\right) = 0. \tag{18}$$

3.1 Stability study

The stability of the obtained fixed points for the simultaneous primary and internal resonance case is determined and studied as follows:

3.1.1 Stability of linear solution

To determine the stability of the linear solution, one investigates the solution of the linearized form of Eq. (11) as

$$A_0' + \mu_1 A_0 = 0 \quad \text{and} \quad B_0' + \mu_2 B_0 + \mathrm{jF}\exp(j\sigma_2 T_2) = 0. \tag{19}$$

Let us consider $A_0(T_2)$ and $B_0(T_2)$ in the form

$$A_0\,(T_2) = \left(\mathrm{p}_1 + \mathrm{jq}_1\right)\exp(j\sigma_1 T_2) \quad \text{and} \quad B_0\,(T_2) = \left(\mathrm{p}_2 + \mathrm{jq}_2\right)\exp(j\sigma_2 T_2), \tag{20}$$

where $\mathrm{p}_1, \mathrm{q}_1, \mathrm{p}_2$ and q_2 are real functions. Substituting Eq. (20) into (19) and separating real and imaginary parts, one obtains

$$\mathrm{p}_1' + \mu_1 \mathrm{p}_1 - \sigma_1 \mathrm{q}_1 = 0 \quad \text{and} \quad \mathrm{q}_1' + \mu_1 \mathrm{q}_1 + \sigma_1 \mathrm{p}_1 = 0, \tag{21}$$

$$\mathrm{p}_2' + \mu_2 \mathrm{p}_2 - \sigma_2 \mathrm{q}_2 = 0 \quad \text{and} \quad \mathrm{q}_2' + \mu_2 \mathrm{q}_2 + \sigma_2 \mathrm{p}_2 + \mathrm{F} = 0. \tag{22}$$

The eigenvalues of the above system of Eqs. (21) and (22) are determined as follows:

$$\lambda = -\mu_1 \pm j\sigma_1 \quad \text{and} \quad \lambda = -\mu_2 \pm j\sigma_2. \tag{23}$$

Consequently, the linear solution is asymptotically stable for all negative values of the obtained eigenvalues.

3.1.2 Stability of nonlinear solution

Now, to determine the stability of the nonlinear fixed point solution of Eqs. (12) and (13), let

$$a = a_0 + a_1, \quad b = b_0 + b_1, \quad \theta_1 = \theta_{10} + \theta_{11} \quad \text{and} \quad \theta_2 = \theta_{20} + \theta_{21}, \tag{24}$$

where a_0, b_0, θ_{10} and θ_{20} are the steady state values, and a_1, b_1, θ_{11} and θ_{21} are the perturbation values. By using Eq. (24), we can reform Eqs. (12) and (13) into the following ones:

$$a_1' = -\left(\mu_1 + L_1 b_0^2 \sin\theta_{10}\right) a_1 - \left(2L_1 a_0 b_0 \sin\theta_{10}\right) b_1 - \left(L_1 a_0 b_0^2 \cos\theta_{10}\right)\theta_{11}, \tag{25.1}$$

$$\theta_{11}' = -\left(3K_1 a_0 + \frac{b_0^2 K_2}{a_0} - \frac{(2\sigma_1 + \sigma_2)}{a_0} + \frac{b_0^2 L_1 \cos\theta_{10}}{a_0}\right) a_1 - 2\left(K_2 b_0 + L_1 b_0 \cos\theta_{10}\right) b_1 + \left(L_1 b_0^2 \sin\theta_{10}\right)\theta_{11}, \tag{25.2}$$

$$b_1' = \left(2L_2 a_0 b_0 \sin\theta_{10}\right) a_1 - \left(\mu_2 - L_2 a_0^2 \sin\theta_{10}\right) b_1 + \left(L_2 b_0 a_0^2 \cos\theta_{10}\right)\theta_{11} + \left(F\cos\theta_{20}\right)\theta_{21} \tag{26.1}$$

$$\theta_{21}' = -2\left(K_4 a_0 + L_2 a_0 \cos\theta_{10}\right) a_1 - \left(3K_3 b_0 - \frac{\sigma_2}{b_0} + \frac{a_0^2 K_4}{b_0} + \frac{a_0^2 L_2 \cos\theta_{10}}{b_0}\right) b_1 + \left(L_2 a_0^2 \sin\theta_{10}\right)\theta_{11} - \left(\frac{F}{b_0}\cos\theta_{20}\right)\theta_{21}, \tag{26.2}$$

The above system are first-order autonomous ordinary differential equations, and the stability of a particular fixed point with respect to an infinitesimal disturbance proportional to $\exp \lambda T_2$ is determined by the eigenvalues of the Jacobian matrix of the right hand sides of Eqs. (25) and (26). The zeros of the characteristic equation are given by

$$\lambda^4 + \mathrm{r}_1\lambda^3 + \mathrm{r}_2\lambda^2 + \mathrm{r}_3\lambda + \mathrm{r}_4 = 0, \tag{27}$$

where, r_1, r_2, r_3 and r_4 are functions of the system parameters. According to the Routh–Hurwitz criterion the necessary and sufficient conditions for all the roots of Eq. (27) to posses negative real parts are

$$\mathrm{r}_1 > 0, \quad \mathrm{r}_1\mathrm{r}_2 - \mathrm{r}_3 > 0, \quad \mathrm{r}_3\left(\mathrm{r}_1\mathrm{r}_2 - \mathrm{r}_3\right) - \mathrm{r}_1^2\mathrm{r}_4 > 0, \quad \mathrm{r}_4 > 0. \tag{28}$$

4 Numerical results

To study the behavior of the system of Eqs. (2), the Runge–Kutta fourth-order method was applied to determine the numerical solution of the given system.

Figure 2 illustrates the response and the phase plane for the nonresonant system at some practical values of the equation parameters. It is observed from this figure that the oscillation response of the first mode starts with increasing amplitude and becomes stable, while the response of the second mode starts with increasing chaotic motion and becomes stable. The worst resonance case is also confirmed numerically as shown in Fig. 3. From this figure we have that the amplitude of the first mode is increased to about 750% with chaotic motion, while the amplitude of the second mode is increased to about 800% and becomes stable.

4.1 Response curves and effects of different parameters

In this Section, the steady state response of the given system at various parameters near the simultaneous primary and internal resonance case is investigated and studied. The frequency response equations given by Eqs. (16), (17) and (18) are solved numerically at the same values of the parameters given in Fig. 2. From the obtained figures, we observe that the solid lines stand for the stable solution and the dashed lines for the unstable solution.

From Fig. 4a, we have the steady state amplitude a of the first mode against the detuning parameter σ_1 which has multi-valued solutions where the jump phenomenon exists. Figures 4b, f show that the steady state amplitude a is a monotonically decreasing function in the nonlinear parameters α_1 and β_2. The instability interval of the trivial solution ($a = 0$) increases as the nonlinear parameter α_1 increases, while the instability interval of this trivial solution decreases as the nonlinear parameter β_2 increases and is shifted to the right. Also, the steady state amplitude a is a monotonically increasing function in the nonlinear parameters α_2 and α_3, and the instability interval of the trivial solution ($a = 0$) increases as the nonlinear parameters α_2 and α_3 increase

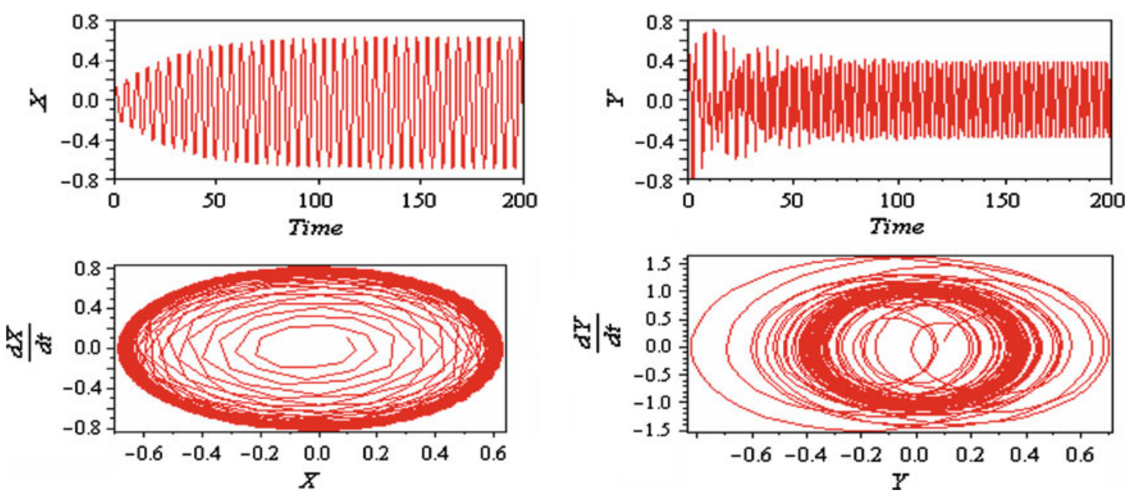

Fig. 2 Nonresonance system behavior (basic case). $\mu_1 = 0.0002, \mu_2 = 0.03, \alpha_1 = 0.2, \alpha_2 = 0.25, \alpha_3 = 0.003, \alpha_4 = 0.004, \beta_1 = 0.3. \beta_2 = 0.35, \beta_3 = 0.004, \beta_4 = 0.005, f = 1.0, \Omega = 2.75, \omega_1 = 1.2, \omega_2 = 1.5$

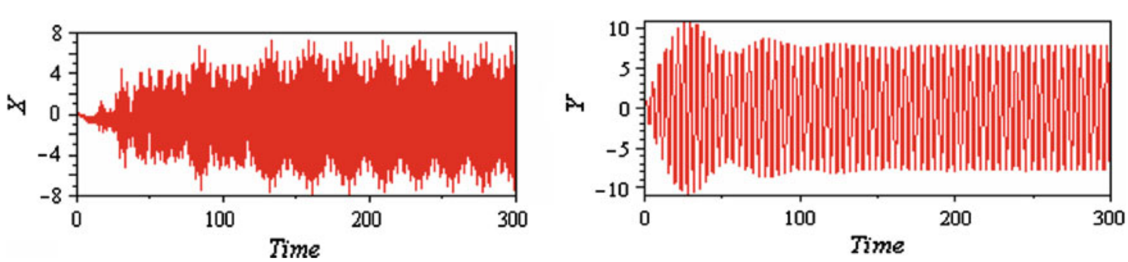

Fig. 3 Simultaneous primary and internal resonance case ($\Omega \cong \omega_2, \omega_2 \cong \omega_1$)

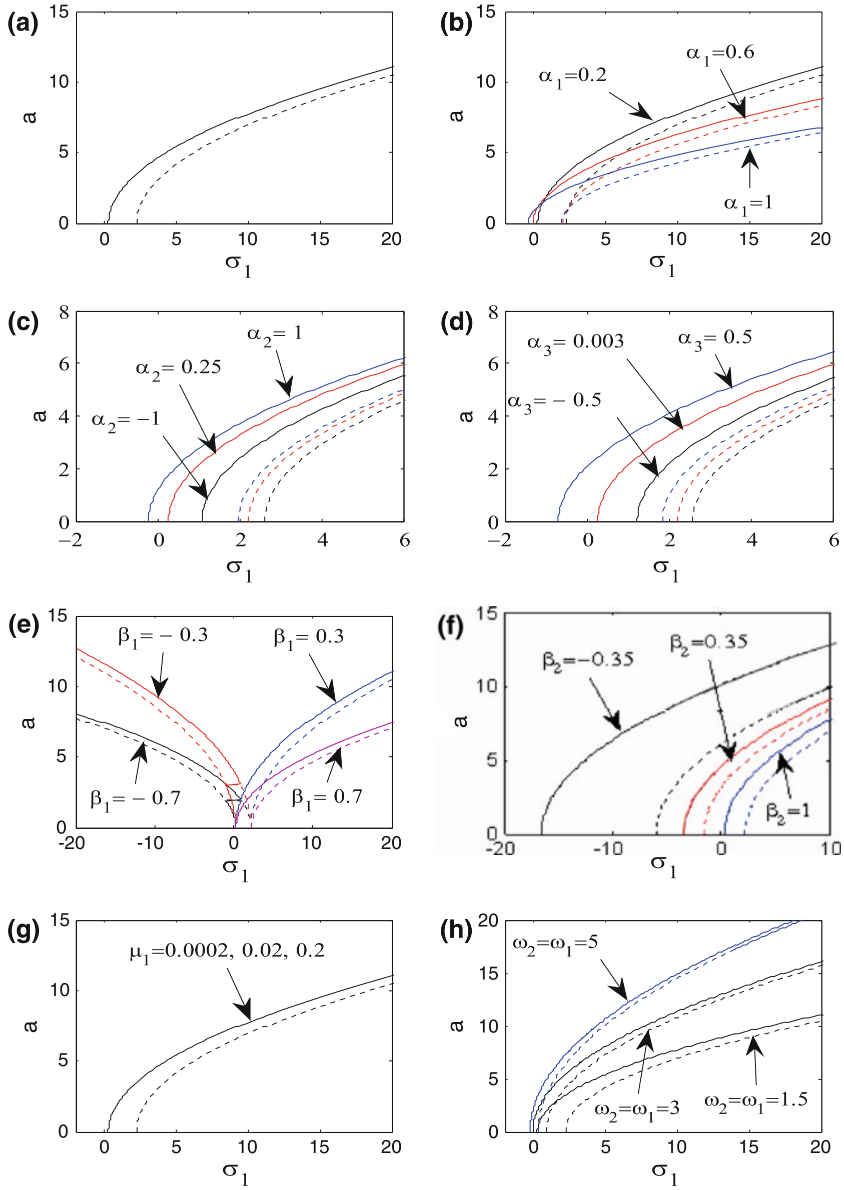

Fig. 4 **a** Effects of the detuning parameter σ_1. **b** Effects of the nonlinear parameter α_1. **c** Effects of the nonlinear parameter α_2. **d** Effects of the nonlinear parameter α_3. **e** Effects of the nonlinear parameter β_1. **f** Effects of the nonlinear parameter β_2. **g** Effects of the damping coefficient μ_1. **h** Effect of the natural frequencies ω_1, ω_2

and are shifted to the left as shown in Fig. 4c, d. For positive and negative values of β_1, the curves are bent to either the right or the left indicating hardening or softening-type nonlinearity and leading to multi-valued solutions (see Fig. 4e). The effect of the damping coefficient μ_1 is insignificant denoting that the saturation phenomenon exists as shown in Fig. 4g.

From Fig. 4h, we find that the steady state amplitude a is a monotonically increasing function in the natural frequencies ω_1 and ω_2, and the instability interval of the trivial solution ($a = 0$) decreases as the natural frequencies ω_1 and ω_2 increase and are shifted to the left.

From Fig. 5a, we have the steady state amplitude b of the second mode against the detuning parameter σ_2 which has multi-valued solutions and the jump phenomenon exists. The effects of the damping coefficient μ_1 and nonlinear parameters α_1, β_1, β_2 and β_4 on the steady state amplitude b are insignificant denoting the occurrence of the saturation phenomenon as shown in Fig. 5b. From the hardening or softening-type nonlinearity for α_2, α_3 and β_3, we have the curve is bent to the right when $\alpha_2 = -5$ or bent to the left when $\alpha_2 = 5$

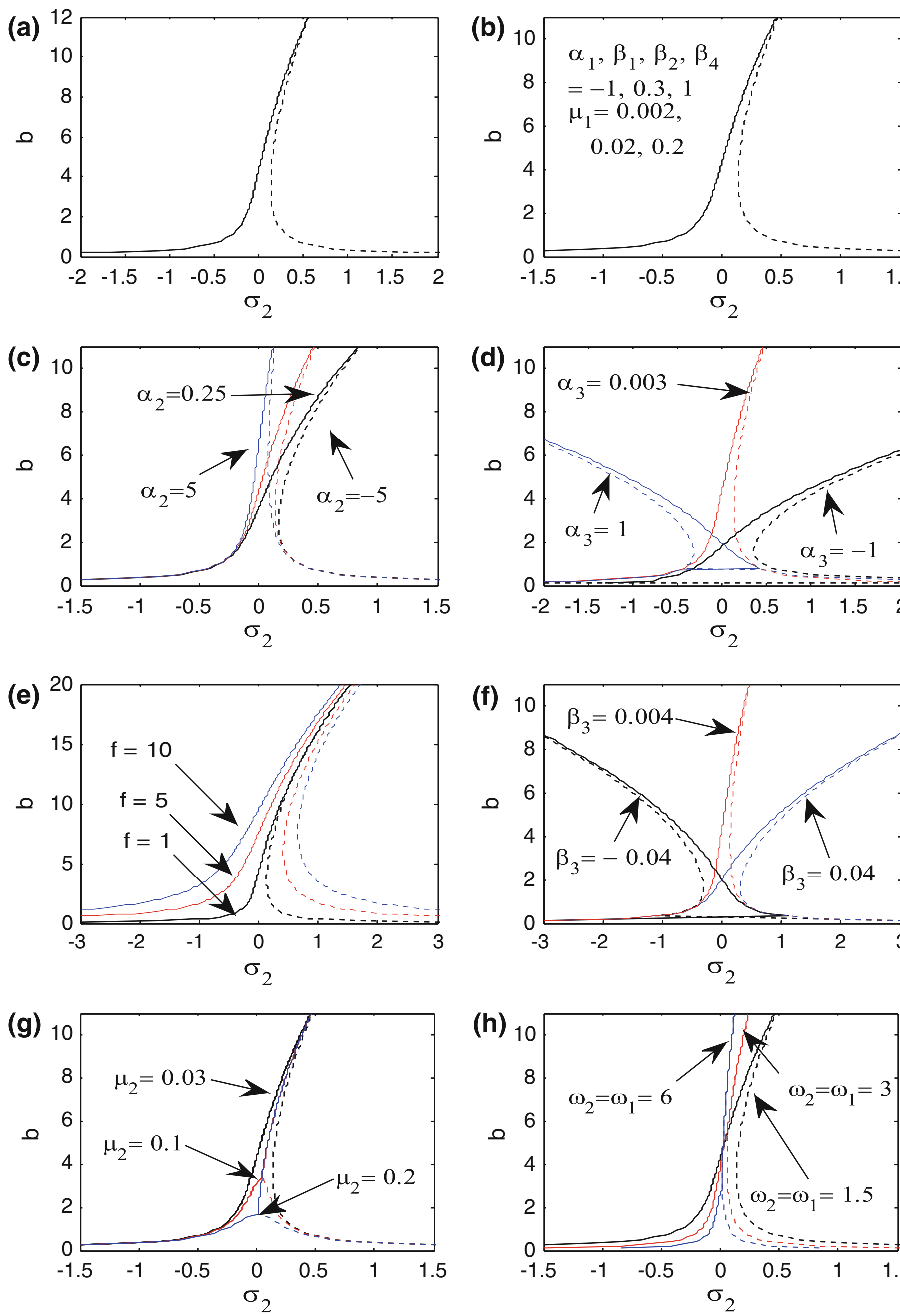

Fig. 5 **a** Effects of the detuning parameter σ_2. **b** Effects of the parameters α_1, β_1, β_2, β_4, μ_1. **c** Effects of the nonlinear parameter α_2. **d** Effects of the nonlinear parameter α_3. **e** Effects of the excitation amplitude f. **f** Effects of the nonlinear parameter β_3. **g** Effects of the damping coefficient μ_2. **h** Effect of the natural frequencies ω_1, ω_2

(see Fig. 5c). Also, the curve is bent to the right when $\alpha_3 = -1$ or bent to the left when $\alpha_3 = 1$ with decreasing value of the steady state amplitude b as shown in Fig. 5d.

For the nonlinear parameters β_3, the curve is bent to the left when $\beta_3 = -0.04$ or bent to the left when $\beta_3 = 0.04$ with decreasing value of the steady state amplitude b as shown in Fig. 5f. These three cases for α_2, α_3 and β_3 lead to multi-valued solutions and the appearance of the jump phenomenon. From Fig. 5e, h, we find that the two branches of the steady state amplitude curve are contracted and give one continuous curve when the values of the excitation force amplitude f are decreased and the values of the natural frequencies ω_1 and ω_2 are increased. Also, the regions of multi-valuedness and stability are decreased. For μ_2 taking

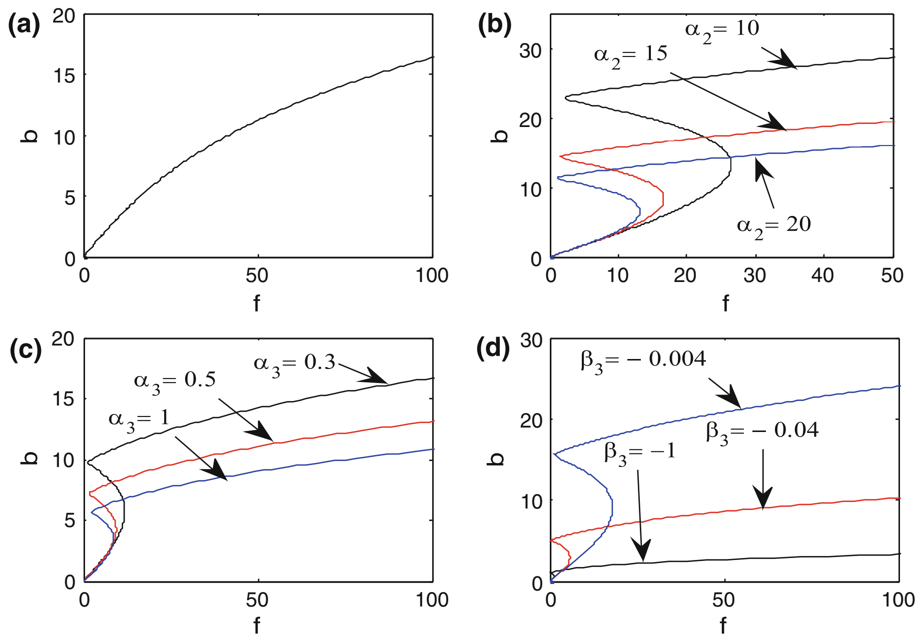

Fig. 6 **a** Effects of the excitation amplitude f. **b** Effects of the nonlinear parameter α_2. **c** Effects of the nonlinear parameter α_3. **d** Effects of the nonlinear parameter β_3

the values (0.03, 0.1 and 0.2), the steady state amplitude b shifts downwards and has decreasing magnitudes, respectively, and the multi-valuedness disappears (see Fig. 5g).

From Fig. 6a, we have that the steady state amplitude b is a monotonically increasing function in f. For increasing the nonlinear parameters α_2 and α_3, we note that the continuous curve shifts downwards and has decreasing stable magnitudes, respectively. The region of multi-valuedness shifts to the left and is defined in small intervals as shown in Fig. 6b, c. From the softening type of nonlinearity of β_3 as shown in Fig. 6d, we find that the continuous curve shifts downwards with decreasing stable magnitudes, and the region of multi-valuedness is contracted. When $\beta_3 = -1$, the zone of multi-valuedness disappears and the continuous curve shifts downwards with decreasing stable magnitudes.

5 Conclusions

Cables are very efficient structural members and hence have been widely used in many long-span structures, including cable-supported bridges, roofs and guyed towers. The method of multiple scales perturbation is applied to analyze the responses of the nonlinear system subjected to harmonic excitation near the primary resonance in the presence of internal resonance which is the worst case. The modulation equations of the amplitude and phase are obtained, and steady state solutions and their stability conditions are determined. The Runge–Kutta fourth-order method is applied to determine the numerical solution of the system of differential equations of the elastic cable, and the worst resonance case is confirmed numerically. From the analysis, the following can be concluded.

For all the system parameters, the multi-valued solutions appear where the jump phenomenon exists for the frequency response curves of the first and second modes. From the frequency response curves of the first mode, we have that the steady state amplitude is a monotonic decreasing function in the nonlinear parameters α_1 and β_2. The instability interval of the trivial solution increases as the parameter α_1 increases and decreases as the parameter β_2 increases and is shifted to the right. For the nonlinear parameters and the natural frequencies $\alpha_2, \alpha_3, \omega_1$ and ω_2, respectively, we find that the steady state amplitude is a monotonically increasing function in $\alpha_2, \alpha_3, \omega_1$ and ω_2, and the instability interval of the trivial solution ($a = 0$) increases as the parameters $\alpha_2, \alpha_3, \omega_1$ and ω_2 increase and is shifted to the left. The hardening or softening-type nonlinearity appears for positive and negative values of the nonlinear parameter β_1, and the steady state amplitude is insignificant for different values of the damping coefficient μ_1.

From the frequency response curves of the second mode, we have that the steady state amplitude is insignificant for different values of the nonlinear parameters α_1, β_1, β_2 and β_4. The curve of the steady state amplitude is bent to the right and bent to the left for negative and positive values of α_2 and α_3, and for positive and negative values of β_3, which indicates hardening or softening-type nonlinearity. Also, the two branches of the steady state amplitude curve are contracted and give one continuous curve when the values of f are decreased and the values of ω_1 and ω_2 are increased and the regions of multi-valuedness and stability are decreased. Furthermore, the steady state amplitude shifts downwards and has decreasing magnitudes, when the values of the damping coefficient μ_2 increase and the multi-valuedness disappears.

From the force response curves, we observe that the steady state amplitude of the second mode is a monotonically increasing function in f. The continuous curve of the steady state amplitude shifts downwards and has decreasing stable magnitudes, when the values of the parameters α_2 and α_3 increase. The region of multi-valuedness shifts to the left and is defined in small intervals. From the softening type of nonlinearity of β_3, the continuous curve shifts downwards with decreasing stable magnitudes, and the region of multi-valuedness is contracted. When $\beta_3 = -1$, the zone of multi-valuedness disappears.

In comparison with the previous work [26], the global bifurcation of this inclined cable leading to primary resonances is investigated. A new global perturbation technique is employed to analyze Shilnikov-type homoclinic orbits and chaotic dynamics in the inclined cable. In our study, the multiple scales perturbation method is applied to analyze the response of the nonlinear system near the obtained worst resonance case (simultaneous principle primary and internal resonance). The stability of the proposed analytic nonlinear solution near the simultaneous primary-internal resonance is studied as well as the effect of some nonlinear parameters on the steady state responses of the vibrating cable leading to multi-valued solutions. The numerical solutions and chaotic response of the nonlinear system of the elastic cable for different parameters are also studied.

Appendix

$$K_1 = \frac{4\alpha_1^2}{3\omega_1^2} + \frac{3\beta_1}{2\omega_1}, \quad K_2 = -\frac{\alpha_1\alpha_2}{\omega_1^3} - \frac{2\alpha_2\alpha_3}{\omega_1} + \frac{\beta_2}{\omega_1}, \quad K_3 = \frac{2\alpha_2\alpha_3\omega_2}{\omega_1^2\left(\omega_1^2 - 4\omega_2^2\right)} + \frac{3\beta_3}{2\omega_2},$$

$$K_4 = \frac{2\alpha_3^2}{\omega_1\left(4\omega_2^2 - \omega_1^2\right)} + \frac{\alpha_1\alpha_3}{2\omega_1^2\omega_2} + \frac{\beta_4}{\omega_2}, \quad L_1 = \frac{\beta_2}{2\omega_1} + \frac{\alpha_2\alpha_3}{\omega_1^2\left(2\omega_2 - \omega_1\right)} - \frac{\alpha_1\alpha_2}{\omega_1\left(\omega_1^2 - 4\omega_2^2\right)},$$

$$L_2 = \frac{\beta_4}{2\omega_2} + \frac{\alpha_1\alpha_3}{6\omega_1^2\omega_2} + \frac{\alpha_3^2}{2\omega_1\omega_2\left(2\omega_2 - \omega_1\right)}, \quad F = \frac{f}{2\omega_2}.$$

References

1. Zhao, Y.Y., Wang, L.H., Chen, D.L., Jiang, L.Z.: Nonlinear dynamics analysis of the two dimensional simplified model of an elastic cable. J. Sound Vib. **255**, 43–59 (2002)
2. Nielsen, S.R., Kirkegaard, P.H.: Super and combinatorial harmonic response of flexible elastic cables with small sag. J. Sound Vib. **251**, 79–102 (2002)
3. Rega, G.: Nonlinear vibrations of suspended cables. Part I: modeling and analysis. J. Appl. Mech. Rev. **57**, 443–478 (2004)
4. Rega, G.: Nonlinear vibrations of suspended cables. Part II: deterministic phenomena. J. Appl. Mech. Rev. **57**, 479–514 (2004)
5. Berlioz, A., Lamarque, C.-H.: A non-linear for the dynamics of an inclined cable. J. Sound Vib. **279**, 619–639 (2005)
6. Kamel, M., Bauomy, H.S.: Nonlinear oscillation of a rotor-AMB system with time varying stiffness and multi-external excitations. J. Vib. Acoust. **131**, 1–11 (2009)
7. Kamel, M., El-Ganaini, W., Hamed, Y.: Vibration suppression in ultrasonic machining described by non-linear differential equations. J. Mech. Sci. Technol. **23**, 2038–2050 (2009)
8. El-Ganaini, W., Kamel, M., Hamed, Y.: Vibration reduction in ultrasonic machine to external and tuned excitation forces. J. Appl. Math. Model. **33**, 2853–2863 (2009)
9. Kamel, M.M.: Nonlinear behavior of Van der Pol oscillators under parametric and harmonic excitations. J. Phys. Scr. **79**, 1–8 (2009)
10. Gattulli, V., Martinelli, L., Perotti, F., Vestroni, F.: Nonlinear oscillations of cables under harmonic loading using analytical and finite element models. J. Comput. Methods Appl. Mech. Eng. **193**, 69–85 (2004)
11. Srinil, N., Rega, G., Chucheepsakul, S.: Two-to-one resonant multi-model dynamics of horizontal/inclined cables. Part I: theoretical formulation and model validation. J. Nonlinear Dyn. **48**, 231–252 (2007)
12. Srinil, N., Rega, G.: Two-to-one resonant multi-model dynamics of horizontal/inclined cables. Part II: internal resonance activation reduced-order models and non-linear normal modes. J. Nonlinear Dyn. **48**, 253–274 (2007)

13. Rega, G., Lacarbonara, W., Nayfeh, A.H., Chin, C.-M.: Multiple resonances in suspended cables: direct versus reduced-order models. Int. J. Nonlinear Mech. **34**, 901–924 (1999)
14. Nayfeh, A.H., Arafat, H.N., Chin, C.-M., Lacarbonara, W.: Multimode interactions in suspended cables. J. Vib. Control **8**, 337–387 (2002)
15. Lacarbonara, W., Rega, G.: Nonlinear normal modes. Part II: activation/orthogonality conditions for shallow structural systems. Int. J. Nonlinear Mech. **38**, 873–887 (2003)
16. Arafat, H.N., Nayfeh, A.H.: Non-linear responses of suspended cables to primary resonance excitations. J. Sound Vib. **266**, 325–354 (2003)
17. Casciati, F., Ubertini, F.: Nonlinear vibration of shallow cables with semiactive tuned mass damper. J. Nonlinear Dyn. **53**, 89–106 (2008)
18. Faravelli, L., Ubertini, F.: Nonlinear state observation for cable dynamics. J. Vib. Control **15**, 1049–1077 (2009)
19. Ubertini F.: Active feedback control for cable vibrations. Int. J. Smart Struct. Syst. **4** (2008)
20. Zhao, Y., Wang, L.: On the symmetric modal interaction of the suspended cable: three-to-one internal resonance. J. Sound Vib. **294**, 1073–1093 (2006)
21. Wang, L., Zhao, Y.: Nonlinear interactions and chaotic dynamics of suspended cables with three-to-one internal resonances. Int. J. Solids Struct. **43**, 7800–7819 (2006)
22. Wang, L., Zhao, Y.: Non-linear planar dynamics of suspended cables investigated by the continuation technique. J. Eng. Struct. **29**, 1135–1144 (2007)
23. Wang, L., Zhao, Y.: Multiple internal resonances and non-planar dynamics of shallow suspended cables to the harmonic excitations. J. Sound Vib. **319**, 1–14 (2009)
24. Kevorkian, J., Cole, J.: Multiple Scale and Singular Perturbation Methods. Springer, New York (1996)
25. Nayfeh, A.H.: Nonlinear Interactions. Wiley, New York (2000)
26. Chen, H., Xu, Q.: Bifurcation and chaos of an inclined cable. J. Nonlinear Dyn. **57**, 37–55 (2009)